Journal of Solid State Chemistry **146,** 88–95 (1999)
Article ID jssc.1999.8312, available online at http://www.idealibrary.com on IDEAL®

Synthesis and Properties of Lanthanum Sodium Manganate Perovskite Crystals

W. H. McCarroll[1]

Chemistry Department, Rider University, 2083 Lawrenceville Road, Lawrenceville, New Jersey 08648

Ian D. Fawcett and M. Greenblatt

Department of Chemistry, Rutgers, The State University of New Jersey, Piscataway, New Jersey 08854

and

K. V. Ramanujachary

Department of Chemistry and Physics, Rowan University, Glassboro, New Jersey, 08028 and Department of Chemistry, Rutgers, The State University of New Jersey, Piscataway, New Jersey 08854

Received December 24, 1998; in revised form March 16, 1999; accepted April 7, 1999

Crystals up to 4 mm on the edge of sodium-substituted lanthanum manganates with the rhombohedral perovskite structure have been grown for the first time using fused salt electrolysis at 980–1000°C. Cs_2MoO_4–MoO_3 mixtures have been employed as solvents. Substitution of Na for La appears to be limited to about 12 at.%. All the phases prepared have an average Mn valence of 3.26(2) which is a result of decreasing A-site vacancies as the Na content is increased. The Curie and insulator–metal transition temperatures increase with increasing Na content with values of 300–320 K being observed for samples containing 10–12 at.% Na. Magnetoresistance values (5 T field) of ~62% at 300 K with a maximum value of 76% at 280 K were observed for a sample of composition $Na_{0.099}La_{0.889}Mn_{0.996}O_3$.

INTRODUCTION

There has been a renewed interest in perovskite-like phases derived from $LnMnO_3$ (Ln = La, Nd, Pr) because of the discovery of so-called colossal magnetoresistance phenomena (CMR), wherein dramatic decreases in the electrical resistivity occur upon the application of a magnetic field (1–5). For instance, stoichiometric $LaMnO_3$ is a paramagnetic insulator at room temperature, which undergoes an antiferromagnetic transition at low temperature with insulating transport behavior. However, partial replacement of La by an alkaline earth metal ion such as Ca or Sr results in a ferromagnetic ordering with the Curie temperature, T_c, near room temperature (RT) and a concomitant insulator–metal transition, at T_{IM}, which is close to T_c. These substituted phases (at ~20–50 at.% doping) exhibit CMR. A maximum in the magnetoresistance (MR) is observed in the vicinity of T_c/T_{IM} where $MR = 100[\rho(H) - \rho(0)]/\rho(0)$ with $\rho(H)$ and $\rho(0)$ being the resistivity at a given temperature in the presence and absence of an applied magnetic field, respectively. For example, the phase with nominal composition $Sr_{0.17}La_{0.83}MnO_3$ has been reported to have a T_c of 283 K and has a MR value approaching 90% near $T_{IM} = 250$ K (15 T field) (6).

In phases where La is replaced by other rare earth metals, such as Nd or Pr, and the alkaline earth metal content is between 30 and 50 mol%, extremely high CMR values approaching 100% are obtained, albeit at relatively low temperatures (7–10). However, because of potential device applications, much of the recent work has focused on the study of materials that display lower but significant CMR at or near room temperature, in particular, Sr-substituted $LaMnO_3$, often formulated as $La_{1-x}Sr_xMnO_3$. The crystal chemistry, however, is much more complex than that simple formulation implies; both the La- (or A-) cation sites and the Mn (or B) sites may be deficient and in some instances oxygen nonstoichiometry can be induced. The physics of CMR materials is not well understood, although it is clear that in the rare earth perovskite manganates it is linked to a mixed Mn(III)/Mn(IV) valency, the sizes of the A cations, the level of defects on both the A and Mn sites, and the crystallographic symmetry, particularly as these factors

[1]To whom correspondence should be addressed.

0022-4596/99 $30.00

affect the Mn–O–Mn bond lengths and angles (11–15). In the Sr-substituted phases, a minimum Mn(IV) content of at least 17% appears to be required to obtain ferromagnetic, metallic-like phases near 250 K, with progressively higher values required for T_c and T_{IM} at room temperature or above (6, 16–19).

Alternative but relatively less explored systems for room temperature CMR manganates are those in which a portion of the rare earth is replaced by an alkali metal. Such phases were studied over 20 years ago by Voorhoeve and coworkers for their catalytic properties (20). They found for phases of nominal composition $La_{1-x}A_xMnO_3$ (A = Na, K, Rb) that up to 40% of the La could be replaced by K but only to 20% if Na or Rb were used. Gubkin *et al.*, reported on the high-temperature solution growth of $La_{0.9}Na_{0.1}MnO_3$ single crystals with T_c/T_{IM} close to 300 K and MR $\sim$ 30% ($H = 2$ T) near T_c/T_{IM} (21). Alkali-metal-substituted systems, similar to those in Ref. (20), were investigated for their electrical and magnetic properties by Shimura *et al.*, who found ferromagnetism and an associated insulator–metal transition at or near room temperature by the addition of 9–16% mol% Na or K (22). Recently, the synthesis of oxygen-deficient phases in which approximately 50% of the La has been replaced by K or Rb have been reported (23) which display a MR of 20–30% in the vicinity of T_{IM} (260 K for both phases). These appear to be perovskite-related phases, in which the anion deficiency is ordered, and are thus quite different from those reported in Ref. (20, 22). Singh *et al.* (24) have synthesized A-cation and oxygen-deficient phases to which they assigned the general formula $La_{1-x-y}A_xMnO_{3-\delta}$ (A = Na or K) by using a NaCl or KCl flux at 1170 K. The highest $T_c = 300$ K ($T_{IM} = 290$ K) was found for $La_{0.82}Na_{0.13}MnO_{2.93}$. The MR properties of these phases were not studied. Boix *et al.* (25) have recently reported the synthesis of several Na-substituted phases by the acetate method which contain 3–15 at.% Na. Interestingly, these phases all have an average Mn valency of 3.33. T_c and T_{IM} appear to increase with increasing Na content and decreasing Mn-site vacancies.

Most of the above studies of alkali-metal-substituted phases have been carried out on polycrystalline phases. Since MR properties appear to be influenced in part by grain boundary and crystallite size effects (26–30), the availability of good quality single crystals, which would be relatively free of such defects, would be desirable. Previously, the method used to produce large single crystals of perovskite manganates, particularly lanthanum manganates doped with alkaline earths, was the arc-image floating zone method (6, 16–18). However, it is unlikely that this method could be used to produce specimens doped with alkali metals because of the high volatility of the latter at the very high temperatures required for crystal growth. Recently, we reported that single-crystal rare earth manganates could be prepared by fused salt electrolysis using alkali molybdate solvents (31–33) at $\sim$1000°C which demonstrated that controlled substitution of Na and K should be possible. We report here the results for our synthesis efforts on Na-substituted $LaMnO_3$ and a study of the electrical and magnetic properties of the phases formed.

EXPERIMENTAL

The crystals were grown in melts obtained using mixtures of cesium molybdate and molybdenum (VI) oxide to which solute ions were added in the form of Na_2MoO_4, La_2O_3, and $MnCO_3$. The electrolyses were carried out for periods of 1–3 days in yttria-stabilized zirconia crucibles (McDanel Vesuvius) using platinum electrodes at temperatures between 980 and 1000°C. Particular conditions for representative phases obtained are given in Table 1. Further details

TABLE 1
Synthesis Conditions and Analyzed Compositions for Sodium-Substituted Lanthanum Manganates Prepared in Y-Stabilized Zirconia Crucibles Using Cs_2MoO_4–MoO_3 and Na_2MoO_4–MoO_3 Solvents

	Starting molar ratios								
Sample ID	Cs_2MoO_4	Na_2MoO_4	MoO_3	La_2O_3	MnO	Time (h)	I (mA)	T (°C)	Analyzed composition
13-81-2A	7.64	0.14	3.00	1.00	1.90	21	13	990	$Na_{0.014}La_{0.932}Mn_{0.976}O_3$
13-81-3A	7.84	0.73	3.30	1.00	1.74	18	13	990	$Na_{0.041}La_{0.918}Mn_{0.991}O_3$
13-81-5A	5.90	1.65	3.02	1.00	1.85	27	15	990	$Na_{0.077}La_{0.888}Mn_{1.002}O_3$
13-81-6A	5.10	1.65	3.00	1.00	1.85	45	15	985	$Na_{0.074}La_{0.903}Mn_{0.986}O_3$
13-81-7A	5.90	4.38	4.14	1.00	1.65	22	15	990	$Na_{0.101}La_{0.877}Mn_{0.997}O_3$
13-81-9A	5.00	5.00	3.86	1.00	1.90	42	15	985	$Na_{0.119}La_{0.861}Mn_{1.008}O_3$
MB10-5A	5.80	4.55	3.05	1.00	1.55	71	10	980	$Na_{0.099}La_{0.889}Mn_{0.996}O_3$
MB10-7A	5.75	4.80	3.00	1.00	1.60	100	11	990	$Na_{0.113}La_{0.888}Mn_{0.984}O_3$
14-6-1A	—	7.25	3.00	1.00	1.80	28	15	1000	$Na_{0.104}La_{0.881}Mn_{0.998}O_3$
14-6-2CM	—	7.25	3.00	1.00	1.80	51	15–20	1000	$Na_{0.069}La_{0.916}Mn_{1.003}O_3$

Note. All Mn valences were determined by iodometric titration, and the oxygen content has been normalized to a stoichiometry of 3.

regarding the method can be found elsewhere (31–33). Chemical analyses for principal metallic constituents as well as trace constituents such as Y, Zr, and Mo were carried out with a Baird Atomic Model 2070 inductively coupled plasma emission spectrometer (ICP). The results are considered accurate to 1–2%. No analysis for Cs was made since previous experiments had shown that this ion was not incorporated into the perovskite phase (33). The average Mn valence was determined by an iodometric titration employing a dead-stop amperometric end point (34). The values are considered valid to within ± 0.03 units.

Powder X-ray diffraction (PXD) data was obtained using a Rigaku D-Max 2 system. When accurate lattice constants were desired, a silicon internal standard was employed. Graphite monochromatized Cu$K\alpha$ radiation was used throughout. Electrical resistivity measurements on selected crystals were made in a four-point probe configuration. The magnetic susceptibility measurements were carried out on randomly oriented crystals using a Quantum Design SQUID magnetometer (MPMS) between 4 and 350 K ($H = 100$ G). Magnetoresistance was measured between 200 and 400 K and in magnetic fields up to 5 T in the transverse configuration (H perpendicular to I).

RESULTS AND DISCUSSION

Table 1 lists the conditions used for the synthesis of several phases prepared in this experiment. All the products labeled with a suffix A are anode products, the lone cathode product being designated by the suffix CM. The anode products grow as small clusters of intergrown, black crystals having a nominally cubic-like habit. Typically, the crystals have facial areas between 1 and 4 mm^2, although some crystals up to 3–4 mm on the edge have been obtained. A photograph of some of the better crystals is shown in Fig. 1. In general, the crystal size increased with the time of electrolysis. The cathode product, like other manganate cathode products, is poorly crystalline and biphasic. It is mentioned here only to alert the reader to their existence and will not be discussed further. Similar products obtained for Sr-doped lanthanum manganates are discussed in more detail elsewhere (33).

We note (Table 1) that the ratio of Na/La in the melts is increased the amount of Na incorporated into the La manganate also increases. However, a relatively large excess of Na in the melt with respect to La is required to achieve a level of 10–12 at.% Na in the manganate, which appears to be the upper limit for this value under the conditions used here. Our Mn valence determination shows that this value

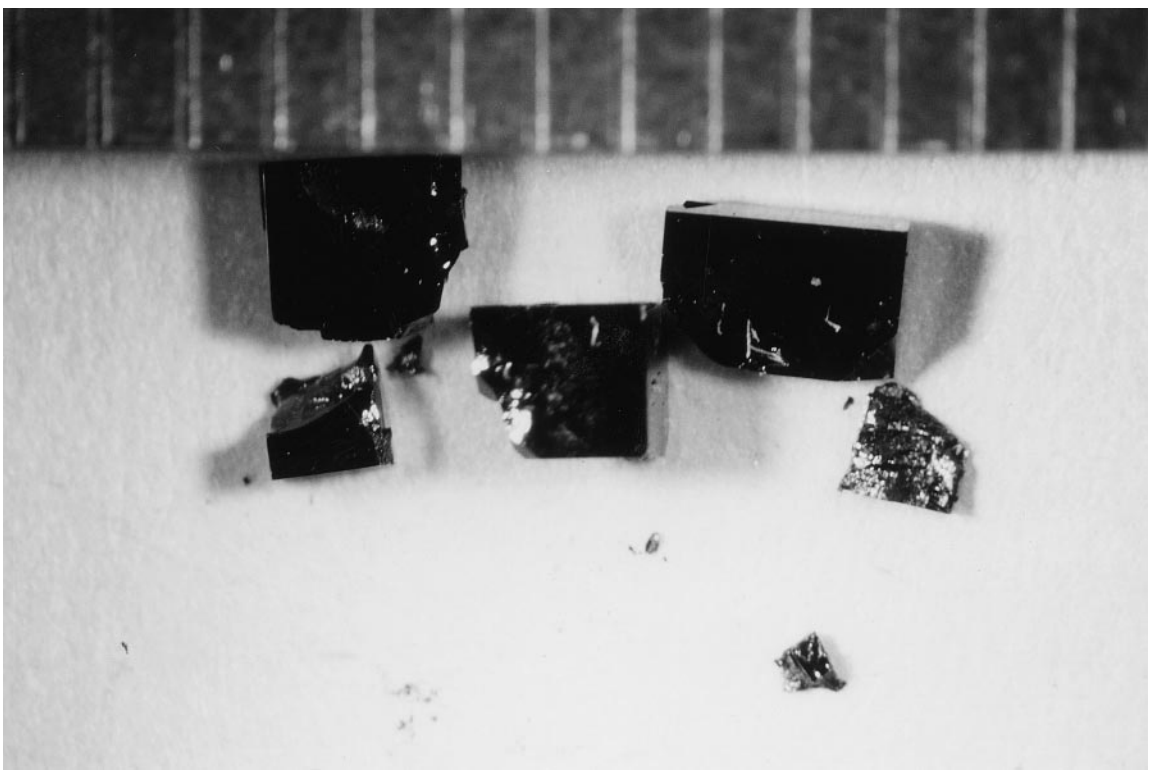

FIG. 1. Photograph of crystal fragments from run MB-10-5A. Scale is in millimeters.

TABLE 2
Unit Cell Data, Analyzed Average Mn Valance, and T_c and T_{IM} Values for Sodium-Substituted Lanthanum Manganates Prepared in Y-Stabilized Zirconia Crucibles using Na_2MoO_4–MoO_3 or Cs_2MoO_4–MoO_3 Solvents

Sample ID	Analyzed composition	a (Å)	α(°)	V_F (Å^3)	Mn val	T_c (K)	T_{IM} (K)	v_A	v_{Mn}
13–44-2A	$La_{0.936}Mn_{0.982}O_3$	5.4816(4)	60.66(1)	59.10(1)	3.25	230	250	0.064	0.018
13-81-2A	$Na_{0.014}La_{0.932}Mn_{0.976}O_3$	5.4802(3)	60.662(6)	59.05(1)	3.27	240	240	0.054	0.024
13-81-3A	$Na_{0.041}La_{0.918}Mn_{0.991}O_3$	5.4782(3)	60.673(6)	59.01(1)	3.23	280	270	0.041	0.009
13-81-6A	$Na_{0.074}La_{0.903}Mn_{0.986}O_3$	5.4758(3)	60.640(5)	58.89(1)	3.27	290	300	0.023	0.014
MB-10-3A	$Na_{0.086}La_{0.903}Mn_{0.986}O_3$	5.4731(3)	60.573(6)	58.71(1)	3.25	280	300	0.011	0.014
MB-10-5A	$Na_{0.099}La_{0.889}Mn_{0.996}O_3$	5.4738(2)	60.631(5)	58.81(1)	3.25	300	300	0.012	0.004
13-81-7A	$Na_{0.101}La_{0.877}Mn_{0.997}O_3$	5.4725(4)	60.624(8)	58.76(1)	3.25	305	300	0.021	0.003
14-6-1A	$Na_{0.104}La_{0.881}Mn_{0.998}O_3$	5.4726(5)	60.600(9)	58.73(1)	3.26	320	—	0.015	0.002
MB-10-7A	$Na_{0.113}La_{0.888}Mn_{0.984}O_3$	5.4709(3)	60.610(6)	58.69(1)	3.27	300	300	—	0.016
13-81-9A	$Na_{0.119}La_{0.861}Mn_{1.008}O_3$	5.4694(3)	60.572(7)	58.60(1)	3.27	310	—	0.020	—
14-6-2CM	$Na_{0.069}La_{0.916}Mn_{1.001}O_3$[a]	5.4781(5)	60.65(1)	58.98(1)	3.18	—	—	0.025	

[a] Sample is biphasic with the main phase being orthorhombic with $a = 5.486$ (7) Å, $b = 7.819$ (8) Å, and $c = 5.524$ (5) Å.

was essentially constant within experimental error at 3.26 ± 0.02, the e.s.d. being well within the estimated uncertainty of the method of ± 0.03 valence units (Table 2).

Our observed valence results are entirely consistent with the decreasing number of A-cation and Mn vacancies (v_A and v_{Mn}, respectively, in Table 2), which occur as the Na content is increased. Finally, we note that V_F, the crystal volume per formula unit (Table 2), decreases as the sodium content increases. This occurs in spite of the fact that the accepted value of the 12-fold crystal radius for Na is slightly larger than that of La, 1.53 vs 1.50 Å (35). Since the Mn valence remains essentially constant, the observed decrease in crystal volume is likely to be the result of decreased electrostatic repulsions within the oxygen sublattice as the cation vacancy concentration decreases. The vacancy level appears to be significantly higher on the A sites than the Mn sites, the latter approaching full stoichiometry, within experimental error, above the 4 at.% Na level.

Figure 2 shows the magnetic susceptibilities as a function of temperature for several of the Na-substituted anode products listed in Table 1. All the phases show a transition to the ferromagnetic state. As expected, the transition temperature, T_c, increases steadily with increasing sodium content (or as the A-cation vacancy level is decreased). The sample with the highest sodium content (11.9 at.%) displayed a T_c of 320 K. The kinks observed below T_c in the temperature-dependent susceptibilities of phases with low sodium content, in particular the phases with 1.4 and 4.1 at.% Na, seem to signal either (i) structural phase transitions, (ii) the onset of complex magnetic interactions, or (iii) possible compositional inhomogeneities. In general, the saturation magnetization decreases with increasing Na content (with a few exceptions, which are probably due to the varying cation vacancy contents). This is to be expected in view of the composition controlled localized to itinerant behavior. Furthermore, since the average valence of Mn remains constant across the samples, it is reasonable to attribute the loss in the saturation magnetization to the decreased number of localized electrons at the Mn sites.

Figure 3 shows the variation of T_c as a function A- and Mn-site vacancy levels as estimated from the results of chemical analysis for the various anode products. It is evident from these plots that a decreasing A-site vacancy level correlates well with an increasing T_c. A more pronounced, but less well-defined trend for the Mn-site vacancy level, is also observed. However, this trend is complicated by the fact that, for samples with more than 1.4 at.% Na, the Mn content is near stoichiometry within the estimated

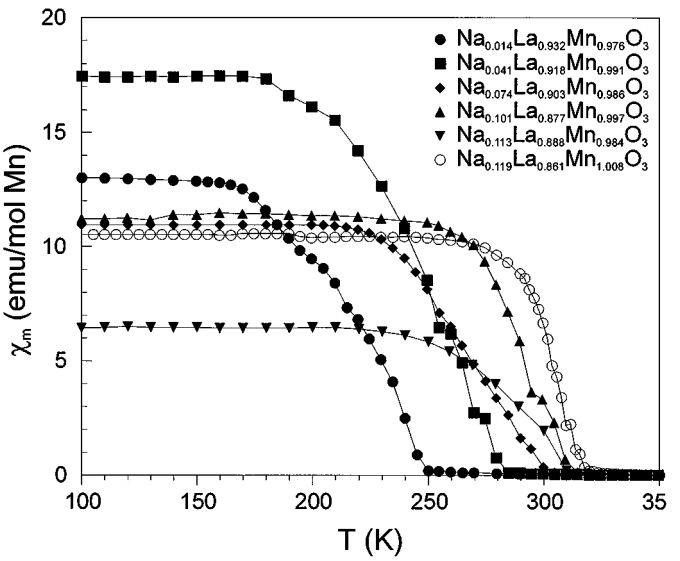

FIG. 2. Magnetic susceptibility vs temperature plots for several Na-doped $LaMnO_3$ samples.

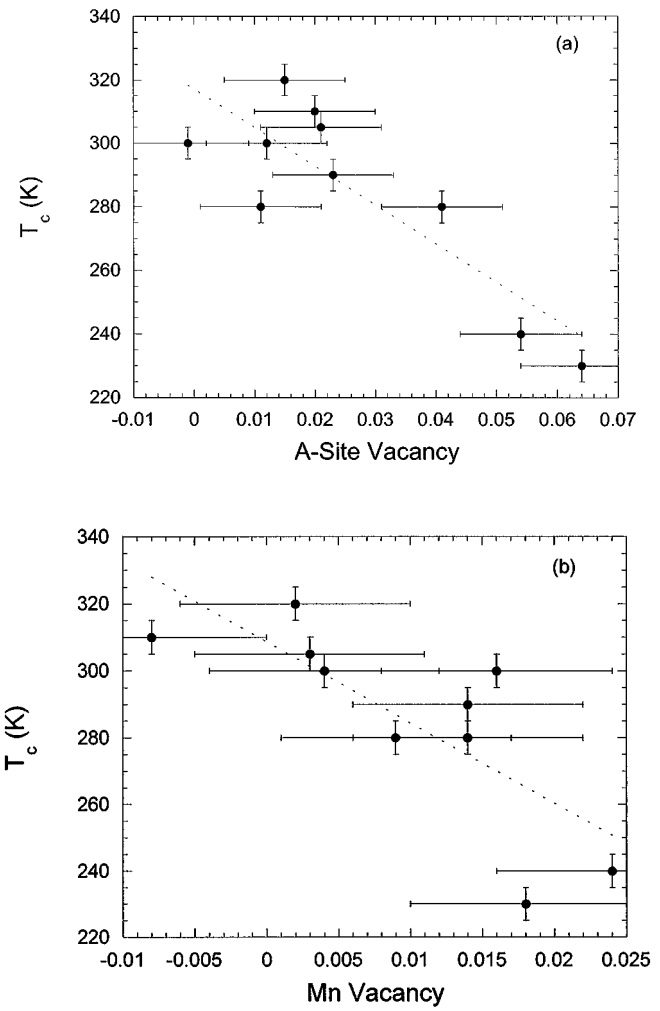

FIG. 3. Plot of Curie temperature vs *A*-site (a) and Mn-site vacancy levels (b). The relative errors in both the T_c's and vacancies (pooled e.s.d. of ± 0.01 for the *A* site and ± 0.008 for the Mn site) are indicated. The straight line drawn in the figures is a guide for the eye.

standard deviation of the analysis (± 0.008, the pooled value for the replicate analysis of 12 different samples).

Given the importance of the Mn–O sublattice for the occurrence of ferromagnetism, vacancies at the Mn site would clearly weaken the exchange correlations and hence T_c would decrease. Furthermore, we propose that vacancies at the *A* site play a secondary role, in that their effect is indirect. For instance, *A*-site vacancies can induce (i) electrostatic repulsions between the O^{2-} ions, thereby increasing the overall cell volume, and (ii) local distortions in the Mn–O–Mn bond angles and distances, both of which will lead to weaker exchange correlations. It is interesting that Boix *et al.* (25) have reported similar correlations between T_c and the level of cation defects, but they considered only Mn-site effects. However, the average Mn valence of their samples is essentially constant but at a value of 3.33 instead of the 3.26 found in our study. The smaller unit cell volumes of their samples compared to ours with similar levels of Na doping is in line with the higher Mn(IV) content of their samples, indicating that we are dealing with two sets of phases with quite different properties. It is clear that Mn vacancies should effect T_c much more than a similar level of *A*-site vacancies. To resolve the effects of the *A*-site defects on the T_c/T_{IM}, in the phases studied here, it would be necessary to grow good quality single crystals with controlled levels of vacancies only at these sites. Unfortunately, the techniques developed so far for the growth of manganate single crystals, including the one reported here, would not permit such a study.

Figure 4a shows the electrical resistivity (at 0 and 5 T) and MR% as a function of temperature for $Na_{0.014}La_{0.932}Mn_{0.976}O_3$ (sample 81-2A). A sharp insulator-to-metal transition with $T_{IM} = 240$ K at zero applied field is observed. At an applied field of 5 T a maximum of 85% in the MR is observed at that same temperature. These observations are similar to those reported previously for $La_{0.936}Mn_{0.982}O_3$ (sample 44-2A) (32). The MR behavior of $Na_{0.074}La_{0.903}Mn_{0.986}O_3$ (81-6A), as shown in Fig. 4b, indicates a maximum of $\sim$60% MR at $\sim$280 K. Figure 4c is a similar plot for sample MB-10-5A with an analyzed composition of $Na_{0.099}La_{0.889}Mn_{0.996}O_3$. Here, the zero field T_{IM} is at 300 K and the maximum MR of 76% is at 280 K (5-T field), which falls off rapidly with temperature. Finally, in Fig. 4d, we show the MR properties of $Na_{0.113}La_{0.888}Mn_{0.984}O_3$ (MB-10-7A), which shows a maximum MR of 55% at 295 K. These MR values are unusually high for the room temperature range and may be related to the overall crystal quality. The sharp decrease in MR below T_{IM} may also be taken as evidence for the lack of grain boundary effects.

The smallest MR is observed in a crystal with the highest sodium content, although there is no particular correlation between the MR and the sodium content. Clearly, the MR is affected by vacancies at the *A* and Mn-sites, T_c of the samples, sharpness of the transition, and the normal-state resistivity of the crystals. Since the average valence of Mn is near optimal for CMR and remained nearly constant across the series, this factor is not responsible for the observed variation in the MR values. On one hand, crystals that are stoichiometric with respect to Mn, but contain relatively large *A*-cation vacancies, exhibit the highest MR values. On the other hand, crystals with the largest Mn deficiencies display relatively smaller MRs, however, at or near RT (Figs. 4b–4d).

Although our crystals appear to be well formed, there does seem to be some small variation from crystal to crystal of the same batch either in regard to the size of the rhombohedral unit cell or perhaps the presence of some crystals with orthorhombic symmetry. The effect is illustrated in

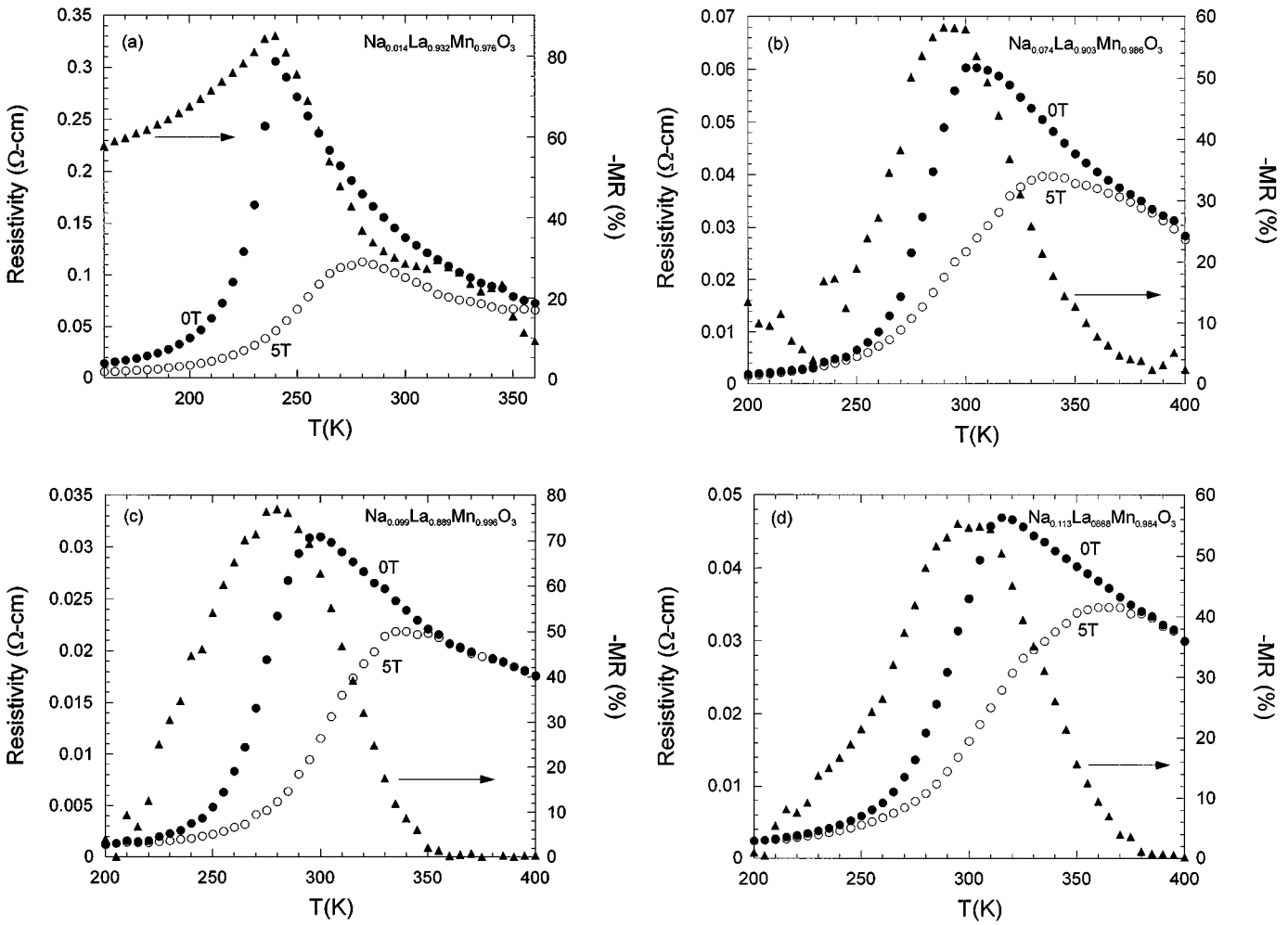

FIG. 4. Resistivity for applied fields of zero and 5T and MR as a function of temperature for (a) $Na_{0.014}La_{0.932}Mn_{0.976}O_3$, (b) $Na_{0.074}La_{0.903}Mn_{0.986}O_3$, (c) $Na_{0.099}La_{0.889}Mn_{0.996}O_3$, and (d) $Na_{0.113}La_{0.888}Mn_{0.984}O_3$.

Fig. 5, which is an expanded portion of the X-ray powder diffraction pattern of three different samples which shows the rhombohedral $\bar{2}20$ and 242 reflections near 68 and 68.5° 2θ, respectively. Figure 5a is for a powder sample prepared from a single-crystal fragment taken from sample 81-3A with an average-analyzed composition of $Na_{0.041}La_{0.918}Mn_{0.991}O_3$. The pattern shows that both reflections have similar sharpness and line widths. Figure 5b is for a powder prepared from a random collection of crystals of the same sample batch and shows a slight, incipient broadening of the $\bar{2}20$ reflection as compared to the 242 reflection. Finally, Fig. 5c obtained for a powder sample made from several crystals of average composition $Na_{0.101}La_{0.877}Mn_{0.997}O_3$ (81-7A) shows a further loss of definition of the reflection at 68° 2θ in which a multiplet is now evident. These effects might be indicative of the presence of a lower symmetry phase such as the well-established orthorhombic type 2 (15, 36), or the presence of a monoclinic phase of the type described by Maignan *et al.* (37).

Alternatively, the effect may be due to multiple rhombohedral phases of slightly different compositions, since the La/Na ratios in the crystal depend upon the melt composition, which will change as the electrolysis proceeds. Indeed, recent synchrotron X-ray powder diffraction studies of a self-doped lanthanum manganate sample prepared by fused salt electrolysis showed the presence of two rhombohedral phases with slightly different lattice parameters (38). Further, the possibility of intergrowths within the same crystal cannot be excluded. These unanswered questions are now being studied at other laboratories with samples supplied by us.

While our study was in progress, the synthesis of very small single crystals (≤ 0.1 mm on the edge) of $La_{0.82}Na_{0.13}MnO_{2.93}$ was reported (39). A single-crystal

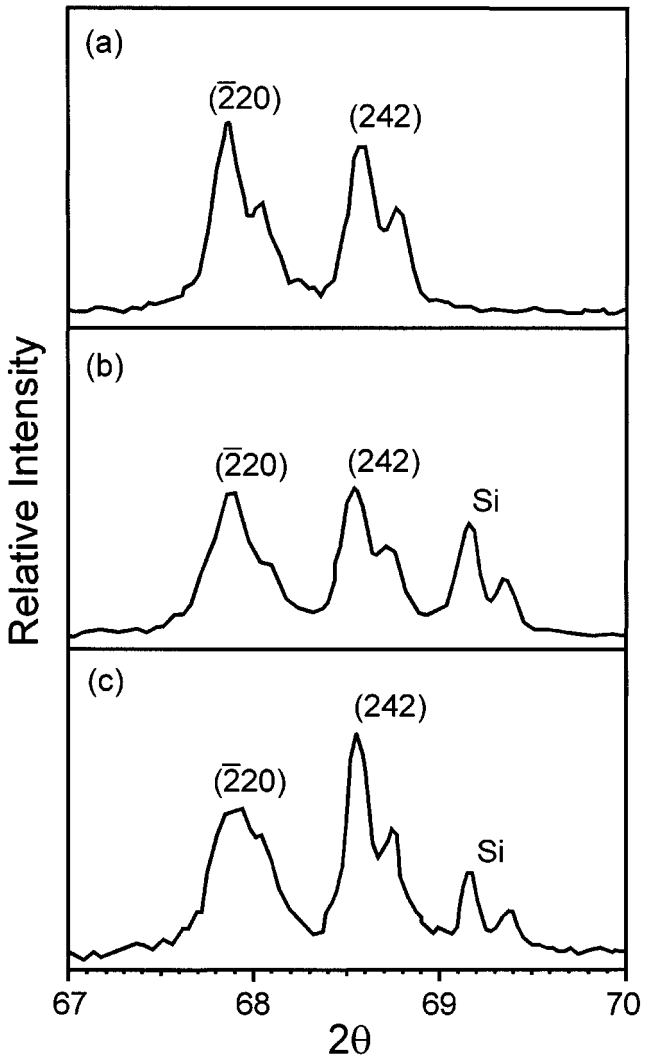

FIG. 5. Powder X-ray diffraction patterns of $Na_{0.086}La_{0.903}Mn_{0.986}O_3$ (MB-10-3A) in the 2θ range of 67–70° (copper radiation). (a) One ground crystal, (b) several ground crystals, and (c) several ground crystals of 13-81-7A, $Na_{0.101}La_{0.877}Mn_{0.997}O_3$.

X-ray diffraction study was consistent with space group $R\bar{3}$ as opposed to the unusual $R\bar{3}c$ found for rhombohedral manganate perovskites. In addition, the unit cell volume was half that of the conventional cell. Although their powder diffraction studies were unable to distinguish between the two space groups, we clearly see a weak line at 2θ near 38°, which is consistent with the larger cell with space group $R\bar{3}c$. Thus, our crystals appear to be fundamentally different from theirs, perhaps as a result of the different method of synthesis.

We have reported previously that the T_c/T_{IM} and MR values of the Sr-substituted lanthanum manganate perovskite single crystals grown by fused salt electrolysis (FSE) are comparable to those, with corresponding composition, grown by zone melting (33). Here, we would like to comment on some of the similarities and differences between the Sr-doped and Na-doped lanthanum manganate crystals, both prepared by fused salt electrolysis. In each of these systems, it is possible to raise the T_c of the self-doped $La_{1-x}Mn_{1-y}O_3$ by a progressive replacement of La with Na or Sr. T_c's as high as 370 K are observed in the $La_{1-x}Sr_xMnO_3$ ($x \sim 0.336$) (33), while the highest T_c observed in the Na system ($x \sim 0.104$) is $\sim$320 K. At low doping levels, both the Sr and Na systems displayed significant vacancies at both the *A* and *B* sites, which generally decreased with increasing dopant content in both systems. The maximum MR attainable in the vicinity of room temperature for the Sr system ($\sim$30–35%) is significantly smaller than the corresponding values seen in the Na system ($\sim$60–80%) when measured under similar magnetic field strengths (5 T). Thus, Na doping appears to be superior to Sr doping for obtaining materials with high MR near RT.

CONCLUSIONS

We have been able to grow crystals of rhombohedral lanthanum manganate perovskites containing up to 12 at.% sodium. Typically, these crystals have facial areas between 2 and 4 mm^2 but crystals up to 4 mm on the edge have been obtained in some instances. An essentially constant average Mn valence of 3.26(2) units was observed for all phases prepared in this study. T_c and T_{IM} increase with an increasing Na content and decreasing *A*-site vacancy level up to $\sim$7 at.% Na. Higher values for Na do not seem to affect T_{IM}, which remain constant at $\sim$300 K. T_c and T_{IM} vary from about 240 K for zero at.% Na to 305–320 K for 10–12 at.% Na substitution. A remarkably high MR value of 62% at 300 K is observed for crystals with approximately 10 at.% Na, which show a maximum MR of 76% at 280 K. Such high values of MR have not been observed previously in bulk manganates in the vicinity of room temperature. These high MR values may be related to the quality of the individual crystals. However, X-ray powder diffraction studies indicate that slight compositional differences may exist for crystals from the same batch. A comparison of the magnetoresistance properties between the Sr- and Na-doped lanthanum manganates prepared by fused salt electrolysis indicates that the nature and role of defects on the MR properties is quite different in each of these systems.

ACKNOWLEDGMENTS

This research was funded in part by NSF-Solid State Chemistry Grant DMR-96-13106. W.H.M. acknowledges with pleasure the assistance of the American Chemical Society Project SEED Scholar Marilyn Baird in some of aspects of this work. K.V.R. acknowledges funding from Research Corporation Grant CC4366.

REFERENCES

1. K. Chahara, T. Ohno, M. Kasai, and Y. Kozono, *Appl. Phys. Lett.* **63,** 1990 (1993).
2. R. von Helmolt, J. Wocker, B. Holzapfel, M. Schultz, and K. Samwer, *Phys. Rev. Lett.* **71,** 2331 (1993).
3. S. Jin, T. H. Tiefel, M. McCormack, R. A. Fastnacht, R. Ramesh, and L. H. Chen, *Science* **264,** 413 (1994).
4. H. L. Ju, C. Kwon, R. L. Greene, and T. Venkatesan, *Appl. Phys. Lett.* **65,** 2108 (1994).
5. M. McCormack, S. Jin, T. H. Tiefel, R. M. Fleming, and J. M. Phillips, *Appl. Phys. Lett.* **64,** 3045 (1994).
6. A. Urushibara, Y. Moritomo, T. Arima, A. Asamitsu, G. Kido, and Y. Tokura, *Phys. Rev. B* **51,** 14103 (1995).
7. A. Maignan, V. Caignaert, Ch. Simon, M. Hervieu, and B. Raveau, *J. Mater. Chem.* **5,** 1089 (1995).
8. B. Raveau, A. Maignan, and V. Caignaert, *J. Solid State Chem.* **117,** 424 (1995).
9. A. Maignan, C. Simon, V. Caignaert, and B. Raveau, *C.R. Acad. Sci. Paris, Ser. IIb* **321,** 297 (1995).
10. J. Wolfman, Ch. Simon, M. Hervieu, A. Maignan, and B. Raveau, *J. Solid State Chem.* **123,** 413 (1996).
11. R. Mahesh, R. Mahendiran, A. K. Raychaudhuri, and C. N. R. Rao, *J. Solid State Chem.* **114,** 297 (1995).
12. H. Y. Wang, S.-W. Cheong, P. G. Radaelli, M. Marezio, and P. Batlogg, *Phys. Rev. Lett.* **75,** 914 (1995).
13. P. Schifffer, A. P. Ramirez, W. Bao, and S.-W. Cheong, *Phys. Rev. Lett.* **75,** 3336 (1995).
14. J. Topfer and J. B. Goodenough, *J. Solid State Chem.* **130,** 117 (1997).
15. N. Sakai and H. Fjellvag, *Acta Chem. Scand.* **50,** 580 (1996).
16. Y. Tokura, A. Urushibara, Y. Moritomo, T. Arima, A. Asamitsu, G. Kido, and N. Furukawa, *J. Phys. Soc. Jpn.* **63,** 3931 (1995).
17. A. Anane, C. Dupas, K. Le Dang, J. P. Renard, P. Veillet, A. M. de Leon Guevara, F. Millot, L. Pinsard, and A. Revcolevschi, *J. Phys. Condens. Matter* **7,** 7015 (1995).
18. H. Kawano, R. Kajimoto, M. Kubota, and H. Yoshizawa, *Phys. Rev. B* **53,** 2202 (1996).
19. J. F. Mitchell, D. N. Argyriou, C. D. Potter, D. G. Hinks, J. D. Jorgensen, and S. D. Bader, *Phys. Rev. B* **54,** 6172 (1996).
20. R. J. H. Voorhoeve, J. P. Remeika, L. E. Trimble, A. S. Cooper, F. J. DiSalvo, and P. K. Gallagher, *J. Solid State Chem.* **14,** 395 (1975).
21. M. K. Gubkin, T. M. Perekalina, A. V. Bykov, and V. A. Chubarenko, *Phys. Solid State* **35,** 728 (1993).
22. T. Shimura, T. Hayashi, Y. Inaguma, and M. Itoh, *J. Solid State Chem.* **124,** 250 (1996).
23. K. Ramesha, V. N. Smolyaninova, J. Gopalakrishnan, and R. L. Greene, *Chem. Mater.* **10,** 1436 (1998).
24. R. N. Singh, C. Shiovakumara, N. Y. Vasanthacharya, S. Subramanian, M. S. Hegde, H. Rajagopal, and A. Sequeira, *J. Solid State Chem.* **137,** 19 (1998).
25. T. Boix, F. Sapina, Z. El-Fadli, E. Martinez, A. Beltrán, J. Vergara, R. J. Ortega, and K. V. Rao, *Chem. Mater.* **10,** 1569, (1998).
26. S. Jin, M. McCormack, T. H. Tiefel, and R. Ramesh, *J. Appl. Phys.* **76,** 6929 (1994).
27. A. Gupta, G. O. Gomg, G. Xiao, P. R. Duncome, P. Lecoeur, P. Trouilloud, Y. Y. Wang, V. P. Dravid, and J. Z. Sun, *Phys. Rev. B* **54,** R15629 (1996).
28. N. D. Mathur, G. Burnell, S. P. Isaac, T. J. Jackson, B.-S. Teo, J. L. MacMansu-Driscoll, L. F. Cohen, J. E. Evetts, and M. G. Blamire, *Nature*, **387,** 266 (1997).
29. H. Y. Hwang, S.-W. Cheong, N. P. Ong, and B. Batlogg, *Phys. Rev. Lett.* **76,** 2041 (1996).
30. H. L. Ju and H. Sohn, *Solid State Commun.* **102,** 463 (1997).
31. W. H. McCarroll, K. V. Ramanujachary, and M. Greenblatt, *J. Solid State Chem.* **130,** 327 (1997).
32. W. H. McCarroll, K. V. Ramanujachary, M. Greenblatt, and F Cosandey, *J. Solid State Chem.* **136,** 322 (1998).
33. W. H. McCarroll, K. V. Ramanujachary, I. Fawcett, and M. Greenblatt, *J. Solid State Chem.* **145,** 88 (1999).
34. F. Licci, G. Turilli, and P. Ferro, *J. Magn. Magn. Mater.* **164,** L268 (1996).
35. R. D. Shannon and C. T. Prewitt, *Acta Crystallogr. B* **25,** 925 (1969); R. D. Shannon, *Acta Crystallogr. A* **32,** 751 (1976).
36. B. C. Hauback, H. Fjellvåg, and N. Sakai, *J. Solid State Chem.* **124,** 43 (1996).
37. A. Maignan, C. Michel, M. Hervieu, and R. Raveau, *Solid State Commun.* **101,** 277 (1997).
38. V. Golovanov and L. Mihaly, private communication.
39. K. Soorynarayana, C. Shivakumara, T. N. Gururow, and M. S. Hegde, *Eur. J. Solid State Inorg. Chem.* **35,** 273 (1998).